

Novel Five-Ring Bent-Core Compounds Exhibiting a Transition from the Electro-optically Nonswitchable to a Switchable B₇ Phase

S. Umadevi and B. K. Sadashiva*

Raman Research Institute, C. V. Raman Avenue, Sadashivanagar, Bangalore-560 080, India

Received February 20, 2006. Revised Manuscript Received August 25, 2006

Two homologous series of achiral five-ring bent-core compounds derived from 2-cyano- or 2-nitro-resorcinol having terminal *n*-alkyl carboxylate groups have been synthesized and characterized. All the compounds investigated show enantiotropic mesophases. Interestingly, the compounds derived from 2-cyano-resorcinol display two mesophases and the higher temperature mesophase shows unusual electro-optical characteristics. In contrast, the nitro-substituted compounds exhibit only one mesophase, which switches electro-optically. This mesophase and the higher temperature phase exhibited by the cyano-substituted compounds show similar characteristics and have been shown to be the same. These observations are unusual but very interesting and represent the first example of a transition from the electro-optically nonswitchable B_{7X} phase to a switchable B_{7FE} phase.

Introduction

The past few years have seen tremendous growth in the investigation of liquid-crystalline phases formed by bent-core compounds. This is due to the rich and unusual phase behavior exhibited by such compounds, in particular, the electro-optical characteristics. The chemical nature of the constituent molecules of such compounds has a significant influence on the observed phase/s and their behavior. Since the first observation¹ of electro-optical switching behavior in achiral bent-core compounds, investigations have been carried out on a very large number of different systems and these have formed the basis of at least three review articles.^{2–4}

Among all the mesophases exhibited by bent-core (BC) compounds, the most beautiful and fascinating textures are shown by the B₇ phase. The B₇ phase was first observed⁵ in 2-nitro-1,3-phenylene bis[4-(4-*n*-alkoxyphenyliminomethyl)benzoates]. Subsequently, this phase was observed⁶ in a number of compounds derived from 2-cyano-resorcinol. The common feature of the B₇ phase exhibited by all these compounds is that the X-ray diffraction (XRD) data are similar. The mesophase shows a medium-angle reflection in addition to several small-angle reflections and of course the diffuse wide-angle reflection. The mesophase is non-switchable even at a fairly high applied voltage and exhibits several beautiful textures. Further, the above general features were seen in a number of other homologous series of

compounds derived from either a 2-nitro- or 2-cyano-resorcinol moiety,^{7,8} containing terminal *n*-alkyl or *n*-alkoxy chain.

There are a number of BC compounds varying in their chemical nature but without the polar cyano or nitro group in the angular position and belonging to different homologous series^{9–12} which exhibit the helical filamentary texture, and in some cases other variants as well, which are assigned the symbol B₇. Typically, these are smectic phases which show either ferroelectric or antiferroelectric switching characteristics and more importantly the medium-angle reflection in the XRD pattern is absent but satellites of weak intensity are seen behind the layer reflections. It has been recommended³ to assign the general symbol B_{7'} to these phases and a detailed analysis of the B₇ phases have been very nicely reviewed.^{3,4} However, it should be pointed out that Coleman et al.¹³ carried out an in-depth analysis of the B_{7'} phase (of MHOBOW) using synchrotron X-ray, micro-beam X-ray, freeze fracture electron microscopy, etc., and proposed a modulated-undulated layer structure for the mesophase based on splay of polarization.

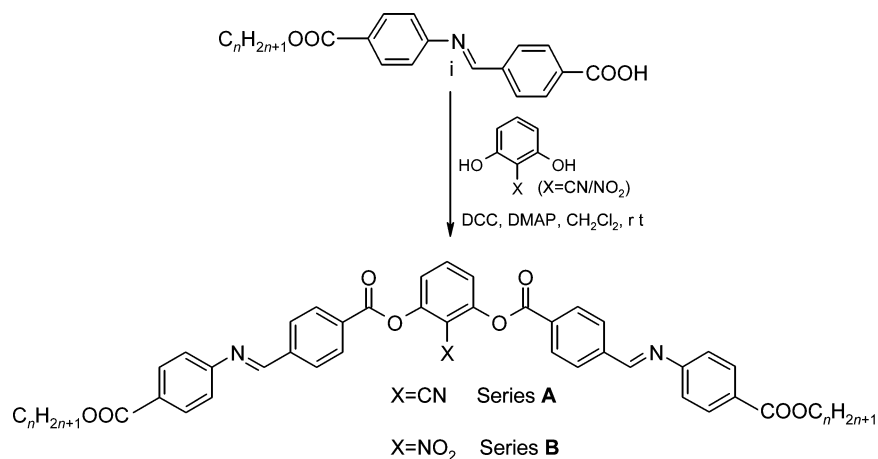
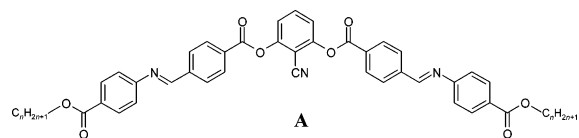
The first observation of a transition from the nonswitchable B₇ mesophase at a higher temperature to an antiferroelectric

* To whom correspondence should be addressed. Tel.: +91 (80) 2361 1015. Fax: +91 (80) 2361 0492. E-mail: sadashiv@rri.res.in.

- (1) Niori, T.; Sekine, T.; Watanabe, J.; Furukawa, T.; Takezoe, H. *J. Mater. Chem.* **1996**, *6*, 1231.
- (2) Pelzl, G.; Diele, S.; Weissflog, W. *Adv. Mater.* **1999**, *11*, 707.
- (3) Amaranatha Reddy, R.; Tschierske, C. *J. Mater. Chem.* **2006**, *16*, 907.
- (4) Takezoe, H.; Takanishi, Y. *Jpn. J. Appl. Phys.* **2006**, *45*, 597.
- (5) Pelzl, G.; Diele, S.; Jakli, A.; Lischka, C.; Wirth, I.; Weissflog, W. *Liq. Cryst.* **1999**, *26*, 135.
- (6) (a) Amaranatha Reddy, R.; Sadashiva, B. K. *Liq. Cryst.* **2002**, *29*, 1365. (b) Amaranatha Reddy, R.; Sadashiva, B. K. *Liq. Cryst.* **2003**, *30*, 273.

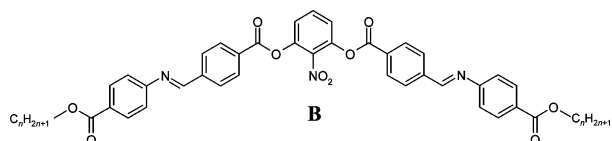
- (7) Weissflog, W.; Nadasi, H.; Dunemann, U.; Pelzl, G.; Diele, S.; Eremin, A.; Kresse, H. *J. Mater. Chem.* **2001**, *11*, 2748.
- (8) (a) Shreenivasa Murthy, H. N.; Sadashiva, B. K. *Liq. Cryst.* **2003**, *30*, 1051. (b) Shreenivasa Murthy, H. N.; Sadashiva, B. K. *J. Mater. Chem.* **2003**, *13*, 2863.
- (9) (a) Heppke, G.; Parghi, D. D.; Sawade, H. *Ferroelectrics* **2000**, *243*, 269. (b) Heppke, G.; Parghi, D. D.; Sawade, H. *Liq. Cryst.* **2000**, *27*, 313.
- (10) Walba, D. M.; Körblova, E.; Shao, R.; Maclennan, J.-E.; Link, D. R.; Glaser, M. A.; Clark, N. A. *Science* **2000**, *288*, 2181.
- (11) Lee, C. K.; Primak, A.; Jakli, A.; Cho, E. J.; Zin, W. C.; Chien, L. C. *Liq. Cryst.* **2001**, *28*, 1293.
- (12) Shankar Rao, D. S.; Nair, G. G.; Krishna Prasad, S.; Anita Nagamani, S.; Yelamagad, C. V. *Liq. Cryst.* **2001**, *28*, 1239.
- (13) Coleman, D. A.; Fernsler, J.; Chattham, N.; Nakata, M.; Takanishi, Y.; Körblova, E.; Link, D. R.; Shao, R.-F.; Jang, W. G.; Maclennan, J. E.; Mondainn-Monval, O.; Boyer, C.; Weissflog, W.; Pelzl, G.; Chien, L.-C.; Zasadzinski, J.; Watanabe, J.; Walba, D. M.; Takezoe, H.; Clark, N. A. *Science* **2003**, *301*, 1204.

Scheme 1. Synthetic Route Followed for the Preparation of Bent-Core Compounds

Table 1. Transition Temperatures (°C) and Associated Enthalpy Values (kJ mol⁻¹) (in Parentheses) for Compounds of Series A^a

compound	n	transition temperatures and enthalpy values
A1	6	Cr 121.0 (4.5) B _{7X} 153.0 (4.5) B _{7FE} 159.5 (24.2) I
A2	7	Cr 120.0 (3.0) B _{7X} 143.0 (3.5) B _{7FE} 161.5 (27.0) I
A3	8	Cr 113.0 (4.0) B _{7X} 137.0 (3.0) B _{7FE} 163.5 (25.5) I
A4	9	Cr 115.5 (6.0) B _{7X} 132.0 (3.0) B _{7FE} 164.5 (27.0) I
A5	10	Cr 118.0 (4.0) B _{7X} 129.0 (4.0) B _{7FE} 165.5 (22.0) I
A6	11	Cr 117.5 (1.5) B _{7X} 129.5 (3.5) B _{7FE} 166.0 (26.5) I
A7	12	Cr 131.5 (24.0) B _{7X} [123.0 (4.0)] ^b B _{7FE} 166.0 (27.0) I
A8	14	Cr 125.5 (80.5) B _{7X} [121.5 (4.0)] ^b B _{7FE} 164.5 (24.5) I
A9	16	Cr 108.0 (75.5) B _{7X} 119.5 (2.0) ^c B _{7FE} 163.0 (19.5) I
A10	18	Cr 107.0 (94.0) B _{7X} 117.0 (1.5) ^c B _{7FE} 161.0 (22.0) I

^a Abbreviations: Cr = crystalline phase, B_{7X} = a nonswitchable mesophase with a two-dimensional lattice, B_{7FE} = a mesophase with a two-dimensional lattice showing ferroelectric switching behavior, I = isotropic phase. ^b Monotropic transition. ^c The phase transition was clearly observed only on cooling from the isotropic phase.

Table 2. Transition Temperatures (°C) and Associated Enthalpy Values (kJ mol⁻¹, in Parentheses) for Compounds of Series B^a

compound	n	transition temperatures and enthalpy values
B1	8	Cr 85.5 (8.3) B _{7FE} 139.0 (24.0) I
B2	9	Cr 93.5 (10.5) B _{7FE} 142.5 (23.0) I
B3	10	Cr 90.0 ^b B _{7FE} 146.0 (24.0) I
B4	11	Cr 89.0 (39.0) B _{7FE} 147.5 (20.5) I
B5	12	Cr 87.5 ^b B _{7FE} 148.0 (20.5) I
B6	14	Cr 83.0 (47.0) B _{7FE} 148.5 (25.0) I
B7	16	Cr 98.0 ^b B _{7FE} 147.5 (22.5) I
B8	18	Cr 81.5 (33.5) B _{7FE} 146.0 (19.0) I

^a See Table 1. ^b Melting point was determined under a polarizing light microscope.

subphase (B_{7AF1}) in a couple of compounds derived from 2-nitroresorcinol was reported^{8(b)} by us. To the best of our knowledge, there is no other example of a switchable B₇ phase obtained from either 2-nitro- or 2-cyanoresorcinol. Very recently, we reported¹⁴ two homologous series of five-

ring bent-core compounds derived from 2-nitro- or 2-cyanoresorcinol. These compounds contain terminal *n*-alkyl carboxylate groups. All the compounds investigated exhibit a nonswitchable B₇ mesophase with all the associated physical properties such as XRD pattern and textural variants. Remarkably, when the orientation of the azomethine linkage group is reversed, a big change occurs in the phase behavior and a switchable B₇ phase is observed. In this paper, we report the synthesis and characterization of the two new homologous series of five-ring BC compounds (series A and series B) derived from the above central units, which exhibit not only the switchable B₇ phase but also a transition to the nonswitchable B₇ phase at a lower temperature for compounds belonging to series A.

Experimental Section

Synthesis. The five-ring symmetrical bent-core compounds were prepared by esterification of 2 equiv of carboxylic acid **1**⁵ with

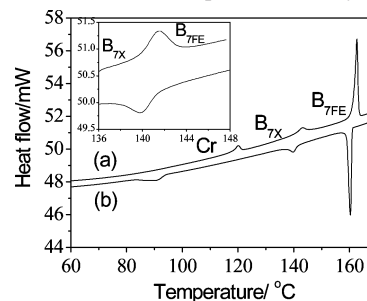


Figure 1. DSC thermogram obtained for compound **A2** at a scan rate of 5 °C min⁻¹: (a) heating cycle; (b) cooling cycle. The inset shows an enlarged view of the mesophase to mesophase transition (scan rate 0.1 °C).

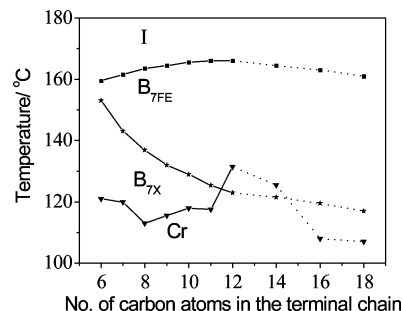


Figure 2. Plot of transition temperature versus number of carbon atoms in the terminal *n*-alkyl chain for compounds of series A. Dotted lines indicate that the data for odd homologues 13, 15, and 17 is not available.

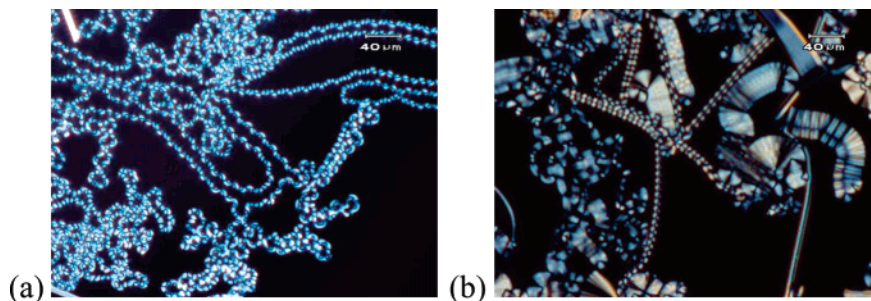


Figure 3. Textural photomicrographs obtained for the B_{7FE} phase of compound **A7** in two different regions; $T = 165$ °C.

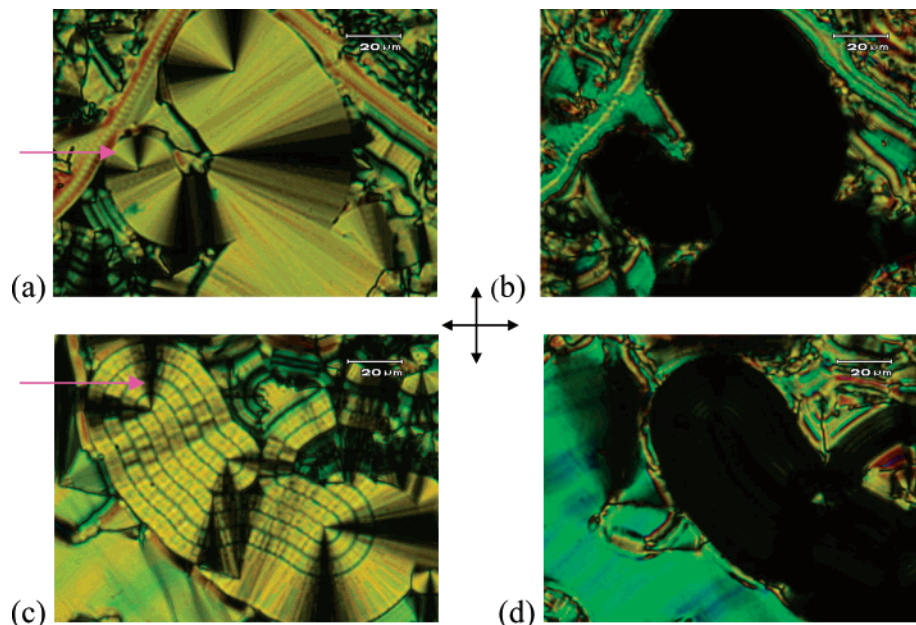


Figure 4. Photomicrographs obtained for compound **A7** showing the textural change after the phase transition $B_{7FE} \rightarrow B_{7X}$ in a cell of thickness $5 \mu\text{m}$ treated for planar alignment: (a) and (c) at $T = 150$ °C; (b) and (d) at $T = 115$ °C (same region as in (a) and (c), respectively).

2-cyanoescorcinol or 2-nitroescorcinol using N,N' -dicyclohexylcarbodiimide (DCC) as coupling reagent and 4-(N,N -dimethylamino)pyridine (DMAP) as catalyst in anhydrous dichloromethane at room temperature. 2-Cyanoescorcinol was prepared following a procedure described by us previously.^{6b} 2-Nitroescorcinol was obtained commercially and used without further purification. The general synthetic pathway used to prepare these compounds is depicted in Scheme 1. A detailed synthetic procedure followed to obtain the compounds is reported elsewhere.¹⁵ A typical procedure followed to prepare compound **A7** and the physical data obtained for the same compound is given below.

2-Cyano-1,3-phenylene Bis[4-(4- n -dodecyloxy-carbonylphenyliminomethyl)benzoate], **A7.** A mixture of 4-(4- n -dodecyloxy-carbonylphenyliminomethyl)benzoic acid, **i** (0.5 g, 1.14 mmol), 2-cyanoescorcinol (0.07 g, 0.57 mmol), DCC (0.25 g, 1.25 mmol), and a catalytic amount of DMAP was stirred at room temperature for 12 h. The precipitated urea was filtered off and washed thoroughly with chloroform. The filtrate was concentrated and the material obtained was crystallized several times using a mixture of chloroform and acetonitrile. Yield 0.45 g (81%), mp 131.5 °C. IR (KBr) ν_{max} : 2922, 2852, 2667, 1745, 1739, 1737, 1712, 1461, 1377, 1280 cm^{-1} . ^1H NMR (400 MHz, CDCl_3): δ 8.55 (s, 2H, $2 \times -\text{CH}=\text{N}-$), 8.38 (d, $^3J = 8.32$ Hz, 4H, Ar-H), 8.11 (d, $^3J = 8.4$ Hz, 4H, Ar-H), 8.09 (d, $^3J = 8.32$ Hz, 4H, Ar-H), 7.77 (t, $^3J = 8.4$ Hz, 1H, Ar-H), 7.49 (d, $^3J = 8.4$ Hz, 4H, Ar-H), 7.26 (d, $^3J = 8.4$ Hz, 2H, Ar-H), 4.33 (t, $^3J = 6.64$ Hz, 4H, $2 \times \text{Ar}-\text{COO}-$

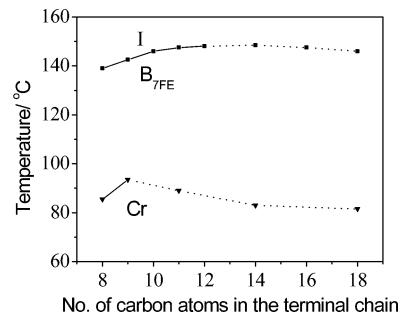


Figure 5. Plot of transition temperature versus number of carbon atoms in the terminal n -alkyl chain for compounds of series **B**. Dotted lines indicate that the data for odd homologues 13, 15, and 17 is not available.

CH_2-), 1.82–1.75 (quin, $^3J = 6.68$ Hz, 4H, $2 \times \text{Ar}-\text{COO}-\text{CH}_2-\text{CH}_2-$), 1.46–1.28 (m, 36H, $2 \times (-\text{CH}_2-)_9$), 0.88 (t, $^3J = 6.48$ Hz, 6H, $2 \times -\text{CH}_3$). $\text{C}_{61}\text{H}_{71}\text{N}_3\text{O}_8$ requires C 75.2, H 7.35, N 4.31; found, C 75.15, H 7.45, N 3.96%.

Equipment and Experiments. All the compounds were purified through repeated crystallization using analytical-grade solvents. The chemical structure of the synthesized compounds was confirmed by a combination of analytical methods. IR spectra were obtained from a Shimadzu FTIR-8400 spectrophotometer. ^1H NMR spectra were recorded on a Bruker AMX 400 spectrometer using tetramethylsilane as an internal standard. Elemental analysis was performed using a Carlo-Erba 1106 elemental analyzer.

The optical textures of the mesophases were observed under an Olympus BX50 polarizing optical microscope equipped with a

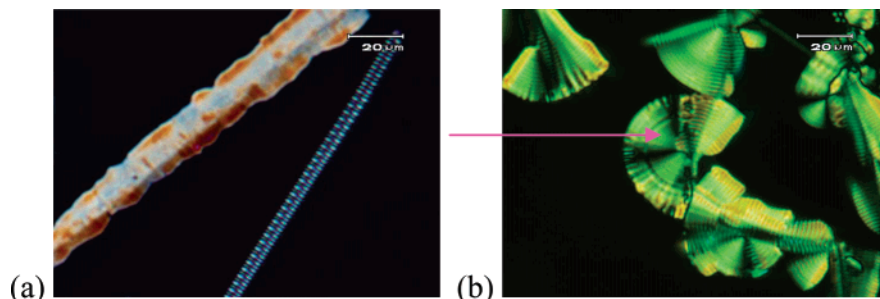


Figure 6. Textural photomicrographs obtained for the B_{7FE} mesophase of compound **B6**; $T = 147$ °C.

Mettler FP82HT hot stage and a Mettler FP90 central processor. Phase transition temperatures and associated enthalpy values were determined from differential scanning calorimetry (DSC) using a Perkin-Elmer calorimeter (Model Pyris 1D) operated at a scanning rate of 5 °C min^{-1} both on heating and cooling cycles. The instrument was calibrated using pure indium as a standard (156.6 °C; $\Delta H = 28.56$ J g^{-1}).

The X-ray diffraction (XRD) measurements on powder samples were carried out using $\text{Cu K}\alpha$ ($\lambda = 1.54$ Å) radiation generated from a 4 kW Rigaku Ultrax-18 rotating anode generator. The beam was monochromated using a graphite crystal. The samples were placed in sealed Lindemann capillaries (diameter: 0.7 mm; wall thickness: 0.01 mm) and in each case the sample temperature was controlled to within ± 0.1 °C. The diffraction pattern of the mesophase was collected on a two-dimensional Marresearch image plate. Electric field experiments were carried out using a standard triangular-wave electric field method.¹⁶ Homemade ITO-coated glass plates without any alignment layers were used for these experiments.

Results and Discussion

Mesomorphic Properties. The transition temperatures and the associated enthalpy values obtained for the compounds of series **A** and series **B** are presented in Tables 1 and 2, respectively.

All the compounds of series **A** are dimorphic. The transition between the mesophases could be detected by calorimetry, although the enthalpy accompanying the transition is relatively small (1.5 – 4.5 kJ mol^{-1}). A DSC thermogram obtained for compound **A2** is shown in Figure 1. Compounds **A1**–**A10** exhibit two mesophases, which are enantiotropic except compounds **A7** and **A8** in which the lower temperature (LT) mesophase is monotropic. One can see that on ascending of the homologous series the thermal range of the higher temperature (HT) phase increases from 6.5 °C for compound **A1** to 44 °C for compound **A10** and, in contrast, the thermal range of the lower temperature phase decreases from 32 °C for **A1** to 10 °C for **A10**. For compounds **A9** and **A10**, transition to the LT phase could not be detected on heating the crystals, but was very clear on the cooling cycle from the HT phase. Microscopic observations also revealed similar behavior. A plot of the transition temperature as a function of the terminal chain length for this series **A** is shown in Figure 2. It can be seen that smooth curve relationships are seen for both the clearing as well as the mesophase–mesophase transitions.

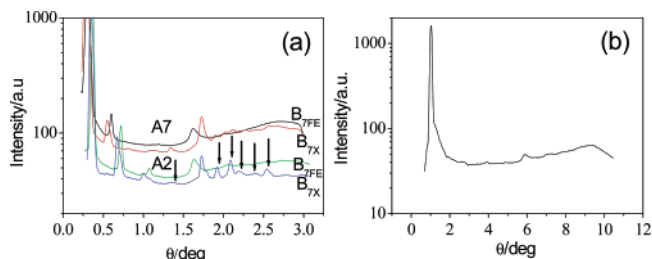


Figure 7. Plots of intensity versus Bragg angle (θ) obtained from the X-ray diffraction pattern. (a) Compound **A2** ($T = 150$ °C, 130 °C) and compound **A7** ($T = 140$ °C, 112 °C); (b) compound **B6** (120 °C).

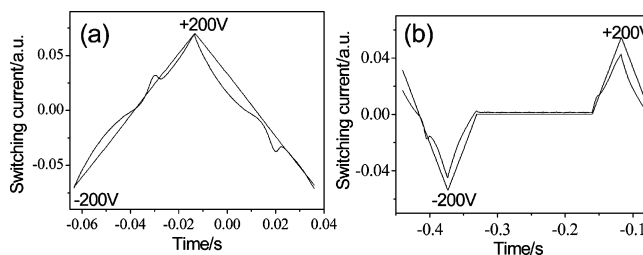


Figure 8. Switching current response trace obtained for the B_{7FE} phase of compound **A7** at 140 °C in an ITO-coated cell of thickness 13.4 μm by applying (a) triangular-wave voltage, 400 V_{pp} , 10 Hz, and (b) modified triangular-wave voltage, 400 V_{pp} , 4 Hz.

All the homologues of this series exhibit similar optical textures when the respective isotropic liquids are cooled slowly, and they resemble those shown by the B_7 phase.^{5–8,14} Helical filaments which are the characteristic feature of the B_7 phase and other patterns obtained on slow cooling of the isotropic liquid of homologue **A7** sandwiched between two glass plates are shown in Figure 3. These textural observations coupled with XRD studies (described later) indicate that the HT phase is indeed the classical B_7 phase. However, the electro-optical studies (described later) showed ferroelectric behavior and hence we have assigned the symbol B_{7FE} to the HT phase. On cooling of this phase further, a transition takes place at 123 °C accompanied by a change in the optical texture that is clearly visible (Figure 4) under the microscope. For example, the myelinic and the smooth fanlike patterns observed in the B_{7FE} phase (Figure 4a,c) became completely dark on phase transition (Figure 4b,d). Interestingly, the birefringence of the texture in other regions increased. The textural changes observed during this phase transition were the same irrespective of whether the glass plates were treated for homeotropic or planar alignment of the sample. This suggests that anchoring conditions do not have any influence on the texture of the mesophase. Since the XRD data of LT phase is almost the same as that of the B_{7FE} phase except for a few additional reflections, and the

(16) Miyasato, K.; Abe, S.; Takezoe, H.; Fukuda, A.; Kuze, E. *Jpn. J. Appl. Phys.* **1983**, *22*, L661.

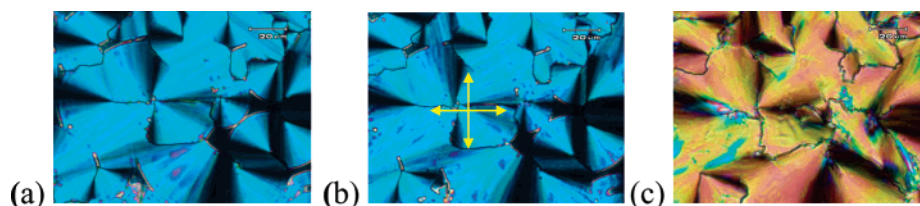


Figure 9. Photomicrographs obtained for the mesophases of compound **A7** on application of triangular-wave electric field: (a) 400 V_{pp}, 10 Hz, 140 °C, B_{7FE} phase; (b) on switching off the field, 140 °C, B_{7FE} phase; (c) 400 V_{pp}, 10 Hz, 120 °C, B_{7X} phase.

phase does not respond to an applied electric field, we have designated this phase as B_{7X}. Similar textural change at the transition was observed for all the other homologues as well.

In complete contrast, the compounds of series **B**, which contain a nitro substituent in the angular position, exhibit only one mesophase. Surprisingly, the melting point of compounds **B3**, **B5**, and **B7** could not be accurately determined from DSC measurements. However, the melting point could be detected under a polarizing light microscope. A plot of transition temperature as a function of the number of carbon atoms in the terminal *n*-alkyl chain for the compounds of series **B** is shown in Figure 5. It is seen that the clearing temperature curve is smooth and is similar to what has been observed for other homologous series exhibiting a B₇ phase, which contain a strongly polar nitro substituent in the angular position. These compounds also exhibit helical filaments and other two-dimensional patterns that are normally associated with a B₇ phase. A couple of such textures obtained for the mesophase of compound **B6** are shown in Figure 6. Compounds **B1**–**B5** also exhibit a texture composed of chiral domains of opposite handedness which we had seen previously¹⁴ in strongly polar compounds. This mesophase has been identified as a B₇ phase on the basis of textural observations and XRD studies.

It is interesting to point out here that the extinction cross obtained in the partial circular domains as well as in the myelinic-like texture (indicated by an arrow in Figure 4a,c and Figure 6b) are parallel to the direction of crossed polarizers. This is similar to the previous observations in the B₇ phase exhibited by strongly polar compounds.^{5–8,14}

XRD Measurements. XRD studies were carried out on powder samples of selected compounds from series **A** and series **B** to obtain information on the phase structure. The XRD pattern of the HT(B_{7FE}) phase of compound **A2** showed several incommensurate Bragg reflections in the small-angle region. This suggests a nonlayered structure for the mesophase. A medium-angle reflection was also observed at around 7.7 Å. This is a characteristic peak typically seen for the B₇ mesophase exhibited by all the compounds derived from 2-cyano-, 2-nitro-, or 5-fluoresorcinol.^{5–8,14,17} A diffuse reflection was observed in the wide-angle region at around 4.2 Å, indicating the fluidity of the phase. When the sample was cooled to the B_{7X} phase, the reflections obtained in the B_{7FE} phase were retained. However, additional reflections were also seen which pointed toward a more ordered mesophase. The X-ray diffractogram obtained in the small-angle region of both the B_{7FE} and B_{7X} phases of

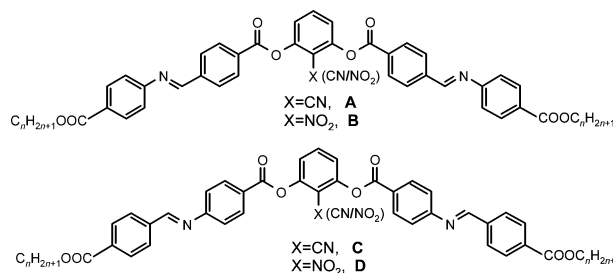


Figure 10. Chemical structure of the compounds used for comparison.

compounds **A2** and **A7** are shown in Figure 7a. The additional reflections obtained in the B_{7X} phase are shown by arrows in this figure. It is interesting to note from this plot that the small-angle reflections in the B_{7X} phase have shifted to slightly lower values (increase in *d*), while the medium-angle reflection has shifted to a higher value (decrease in *d*).

It has been pointed out³ that the distance corresponding to the medium-angle reflection is in the range of typical values of face-to-face packed dimers. Electron-deficient compounds are known to form face-to-face aggregates, whereby the planes of the aromatics are shifted with respect to each other.¹⁸ The compounds exhibiting B₇ phase known so far contain strongly polar electron-withdrawing substituents such as cyano and nitro groups. If a face-to-face packing is assumed in the B₇ phase, then the medium-angle reflection might correspond to some order between these dimers. In the absence of high-resolution XRD data, it would be difficult to interpret the observations.

Although a highly condensed two-dimensional smectic layer structure has been proposed for the B₇ phase of a 2-cyano-substituted compound on the basis of synchrotron X-ray diffraction techniques,¹⁹ the precise structure of the phase is not yet clear. Therefore, it is difficult to speculate about the structure of the phase which exists below the B_{7FE} phase. Since there are a few additional reflections in the XRD pattern as compared to the standard B₇ mesophase,⁵ we have assigned the symbol B_{7X} for the LT phase.

Similar XRD patterns were obtained for the other homologues of series **A**. The XRD patterns obtained for the compounds of series **B** are also similar to the B_{7FE} phase and a typical angular intensity profile obtained for compound **B6** is shown in Figure 7b.

Electric Field Experiments. To investigate the polar properties of the mesophase, electric field experiments were carried out on representative compounds from the two series.

(17) Pelzl, G.; Schröder, M. W.; Dunemann, U.; Diele, S.; Weissflog, W.; Jones, C.; Coleman, D.; Clark, N. A.; Stannarius, R.; Li, J.; Das, B.; Grande, S. *J. Mater. Chem.* **2004**, *14*, 2492.

(18) Hunter, C. A.; Sanders, J. K. M. *J. Am. Chem. Soc.* **1990**, *112*, 5525.
(19) Kang, S.-W.; Amaranatha Reddy, R.; Sadashiva, B. K.; Kumar, S. Presented at the International Liquid Crystal Conference, Ljubljana, July 4–9, Book of Abstracts, 2004, SYN-P141.

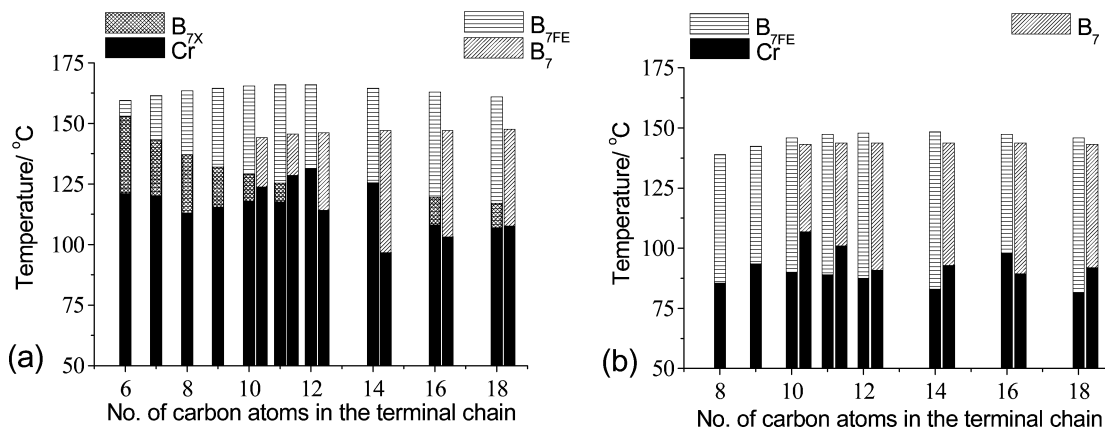


Figure 11. Bar diagram showing a comparison of transition temperature versus the number of carbon atoms in the terminal chain for compounds under investigation and the analogous compounds with reversal of azomethine linkage reported earlier:¹⁴ (a) series A (left column) and series C (right column); (b) series B (left column) and series D (right column).

A sample of compound **A7** was filled into an ITO-coated cell of thickness $13.4 \mu\text{m}$ through capillary action. The sample was cooled from the isotropic state to the mesophase ($T = 140 \text{ }^\circ\text{C}$) and a triangular-wave voltage was applied and slowly increased. At a voltage of $400 \text{ V}_{\text{pp}}$ and a frequency of 50 Hz , a small hump was observed in the current response trace, which became a prominent peak on reducing the frequency (10 Hz). The single peak obtained persisted even on reducing the frequency down to 0.1 Hz , indicating ferroelectric behavior for the mesophase. The ferroelectric nature was supported by the behavior of the mesophase under a modified triangular wave with a plateau at 0 V , during which also only one peak was observed per each half cycle. The peak obtained in the mesophase disappeared on going to the isotropic phase, thus ruling out the possibility of ionic contribution. The current response traces obtained by the application of triangular-wave voltage and modified triangular-wave voltage are given in (a) and (b), respectively, of Figure 8. The spontaneous polarization value estimated from this trace is about 98 nC cm^{-2} . Hence, we have assigned the symbol $B_{7\text{FE}}$ to this HT phase. On cooling of the mesophase further under an electric field ($400 \text{ V}_{\text{pp}}$, 10 Hz), there was a gradual decrease in the peak size, the peak completely disappearing at $122 \text{ }^\circ\text{C}$ ($B_{7\text{X}}$ phase). This indicates that the $B_{7\text{X}}$ phase does not respond to the electric field.

The optical response of the mesophase on application of an electric field was observed under a polarizing microscope. In the $B_{7\text{FE}}$ phase smooth fans as well as circular domains were seen in which the extinction brushes are oriented along the crossed polarizers. This indicates an anticlinic tilt of the molecules in the mesophase. The texture remained the same on reversing the polarity of the applied field as well as on turning off, except for a slight variation in the birefringence. Similar behavior was observed under a dc electric field also. These observations suggest a racemic ferroelectric structure for the mesophase. On transition to the LT phase, a slight change in the texture was observed accompanied by a color change. However, the orientation of the extinction brushes in the circular domains remained the same as that in the $B_{7\text{FE}}$ phase. The photomicrographs obtained under these conditions are shown in Figure 9.

The mesophase exhibited by compounds of series **B** was also found to be polar and exhibit ferroelectric switching

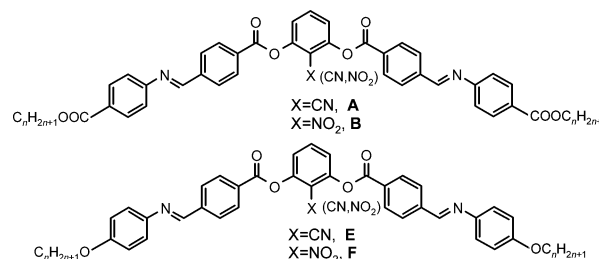


Figure 12. Chemical structure of the compounds used for comparison.

characteristics. For example, the spontaneous polarization value estimated from the current response trace obtained for compound **B2** is about 184 nC cm^{-2} .

It is appropriate to mention here that until now there have been only two examples of switchable B_7 phase obtained from compounds whose central phenyl unit contains a highly polar substituent. These are five-ring Schiff's base bent-core compounds derived from 2-nitroresorcinol^{8b} and 5-fluoro-resorcinol.¹⁷ However, the present work is the first example of a B_7 phase exhibited by bent-core compounds derived from 2-cyanoresorcinol, showing ferroelectric characteristics to an applied electric field and dimorphism as well.

Effect of Orientation of Azomethine Linkage Group.

A comparison (see Figure 10) was made between the compounds of the present two series **A** and **B** and the compounds reported earlier¹⁴ (series **C** and **D**) which differ by the way in which the azomethine linking group is connected. Interestingly, two mesophases were observed for all the compounds of series **A** while compounds 2-cyano-1,3-phenylene bis[4-(4-*n*-alkyloxycarbonylbenzylideneamino)-benzoates] (series **C**) exhibited only one phase. Even more interestingly, two phases are obtained for the compounds of series **A** in which the higher temperature $B_{7\text{FE}}$ phase responds to an applied electric field, which is in complete contrast to those reported¹⁴ previously (compounds **C** exhibit B_7 phase which is nonswitchable). A comparison of the transition temperature versus number of carbon atoms in the terminal chain and the thermal range of the mesophases for the compounds of series **A** and series **C** is shown in Figure 11a as a bar diagram. It can be seen from the graph that, in series **A**, the clearing transition temperatures are increased by about $20 \text{ }^\circ\text{C}$ in addition to inducing an additional switchable phase.

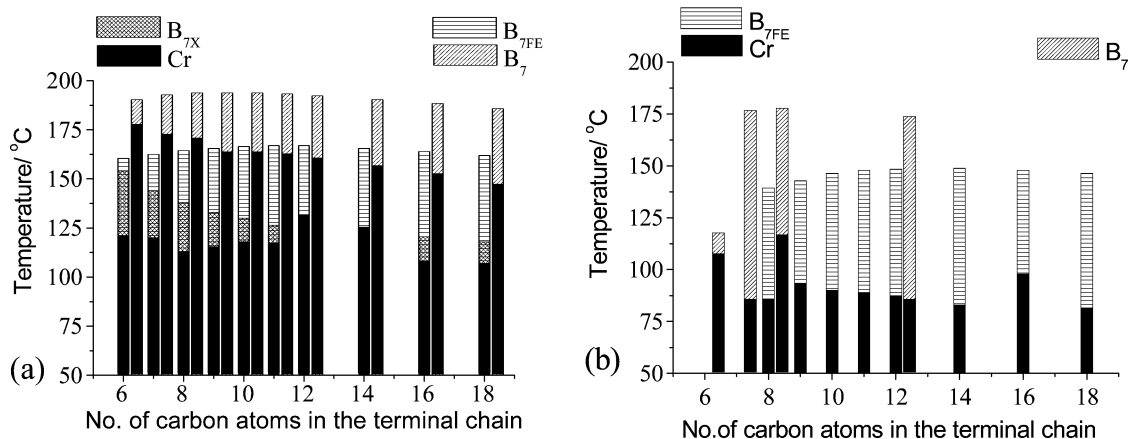


Figure 13. Bar diagram showing a comparison of transition temperatures as a function of number of carbon atoms in the terminal chain: (a) compounds of series **A** (left column) and those of series **E**^{8a} (right column); (b) compounds of series **B** (left column) and standard **B**₇ materials, series **F**⁵ (right column).

A similar comparison was made between the compounds of series **B** and the analogous compounds with the reversal of azomethine linking group reported earlier¹⁴ (compounds **D**). In this case also clearing transition temperatures of the B_{7FE} phase of compounds of series **B** are enhanced, but the increment in the temperature is relatively very small and is about only 3–5 °C. However, the melting points have been reduced by about 10 °C, resulting in an increase in the thermal range of B_{7FE} phase. These differences between these two series of compounds are shown in Figure 11b. Further, B_{7FE} phase of compounds of series **B** exhibits ferroelectric characteristics, while B₇ phase exhibited by compounds **D** is nonswitchable. These observations clearly demonstrate the profound change induced as a result of a small change in the form of orientation of the linking group.

Effect of Terminal Linking Group. A majority of the bent-core compounds contain *n*-alkyl or *n*-alkoxy chains directly attached to the phenyl ring in the terminal position whereas in the present series of compounds *n*-alkyl chain is attached to a carboxyl group. This small change has brought about a drastic change in the mesomorphic behavior as discussed below.

A comparison (see Figure 12) of the mesomorphic properties of compounds of series **A** with the analogous compounds having a terminal *n*-alkoxy chain^{8a} (series **E**) indicates the following interesting features.

Two mesophases are observed for all the compounds of series **A**. The higher temperature B_{7FE} mesophase showed ferroelectric response to an applied electric field whereas the lower temperature phase is nonswitchable. The compounds 2-cyano-1,3-phenylene bis[4-(4-*n*-alkoxyphenyliminomethyl)benzoates] (series **E**) are monomorphic and the B₇ phase exhibited by them do not show any response to an applied electric field at least up to 40 V μm⁻¹.^{8a} Further, melting points and clearing temperatures of compounds of series **A** have been reduced considerably. An increase in the thermal range of switchable (B_{7FE}) phase was also observed. A comparative plot of transition temperature as a function of the number of carbon atoms in the terminal chain is shown as a bar diagram in Figure 13a.

A similar comparative study between the compounds of series **B** and the compounds with the same core but terminal

n-alkoxy chain⁵ (series **F**) again indicates a reduction in melting points as well as clearing transition temperatures. However, the decrease in the melting points is relatively small. A comparative bar diagram of transition temperature as a function of the number of carbon atoms for the compounds of series **B** and those of series **F** is shown in Figure 13b.

Conclusions

Two novel series of achiral five-ring bent-core compounds derived from 2-cyano- and 2-nitroresorcinol containing *n*-alkyl carboxylate groups in the terminal positions were synthesized and their mesomorphic properties investigated. All these compounds exhibit a B₇ phase, which show ferroelectric switching characteristics. In addition, homologues of 2-cyano-substituted compounds displayed a transition from a switchable (B_{7FE}) phase to a nonswitchable (B_{7X}) mesophase as the temperature was lowered. This is the first observation of dimorphism of the B₇ phase in which the higher temperature phase (B_{7FE}) is electro-optically switchable and the lower temperature phase (B_{7X}) is nonswitchable, and the compounds are derived from 2-cyanoresorcinol. In addition, the B₇ phase observed in compounds derived from 2-nitroresorcinol is monomorphic and responds to an applied electric field and this phase and the higher temperature phase of cyano-substituted compounds are the same. These mesophases show the medium-angle reflection in the XRD pattern displayed by the B₇ mesophase of original materials.

Acknowledgment. The authors wish to thank Ms. K. N. Vasudha for technical support and the NMR Research Center, Indian Institute of Science, Bangalore, for recording the NMR spectra.

Supporting Information Available: The analytical and spectral data obtained for compounds **A1–A6** and **A8–A10** and for compounds **B1–B8** and the *d*-spacings obtained in the small-angle region for the mesophase of compounds of series **A** and **B** are collected in Table 3. This material is available free of charge via the Internet at <http://pubs.acs.org>.